Pancreatic Islet Vasculature Adapts to Insulin Resistance Through Dilation and Not Angiogenesis

Chunhua Dai,[1] Marcela Brissova,[1] Rachel B. Reinert,[1] Lara Nyman,[1] Eric H. Liu,[2] Courtney Thompson,[1] Alena Shostak,[1] Masakazu Shiota,[3] Takamune Takahashi,[4] and Alvin C. Powers[1,3,5]

Pancreatic islets adapt to insulin resistance through a complex set of changes, including β-cell hyperplasia and hypertrophy. To determine if islet vascularization changes in response to insulin resistance, we investigated three independent models of insulin resistance: *ob/ob*, GLUT4$^{+/-}$, and mice with high-fat diet–induced obesity. Intravital blood vessel labeling and immunocytochemistry revealed a vascular plasticity in which islet vessel area was significantly increased, but intraislet vessel density was decreased as the result of insulin resistance. These vascular changes were independent of islet size and were only observed within the β-cell core but not in the islet periphery. Intraislet endothelial cell fenestration, proliferation, and islet angiogenic factor/receptor expression were unchanged in insulin-resistant compared with control mice, indicating that islet capillary expansion is mediated by dilation of preexisting vessels and not by angiogenesis. We propose that the islet capillary dilation is modulated by endothelial nitric oxide synthase via complementary signals derived from β-cells, parasympathetic nerves, and increased islet blood flow. These compensatory changes in islet vascularization may influence whether β-cells can adequately respond to insulin resistance and prevent the development of diabetes. ***Diabetes*** **62:4144–4153, 2013**

Pancreatic islets are highly vascularized, and this feature is critical for β-cells to rapidly sense the blood glucose and secrete insulin into the systemic circulation (1,2). Islet vascularization begins early in pancreas development and is maintained in adulthood as a consequence of islet cell production of angiogenic factors such as vascular endothelial growth factor-A (VEGF-A) and angiopoietin-1 (Ang-1) (3–6). These factors recruit endothelial cells (ECs), stimulate blood vessel growth and maturation, and in the case of VEGF-A, promote formation of EC fenestrations (5,6). In addition, ECs adjacent to pancreatic epithelium reciprocally influence islet cell differentiation and development (7,8).

β-Cells have a remarkable ability to respond to changes in an organism's metabolic state, such as changes in the blood glucose or increased insulin requirements. For example, when insulin resistance develops, β-cells of the pancreatic islet can dramatically increase insulin production and secretion with an increase of β-cell mass, thus maintaining normoglycemia (9,10). In this way, mouse models with marked insulin resistance and humans with obesity-related insulin resistance are hyperinsulinemic but not hyperglycemic. The mechanisms underlying this β-cell adaptation to insulin resistance and their subsequent failure in some individuals who develop type 2 diabetes are incompletely understood.

Because of the highly vascularized state of pancreatic islets and the marked changes in β-cell size and number in the setting of insulin resistance, we hypothesized that the islet vasculature must adapt to these changes in β-cell mass and insulin requirements. We envisioned that a hyperplastic islet, like a growing tumor mass, would increase production of angiogenic factors to increase its vascular supply with expanding β-cell mass (11). To test this hypothesis, we examined islet vascularization in three mouse models of insulin resistance and found, unexpectedly, that islet vessel density was decreased, not increased, and that the intraislet vasculature became markedly dilated whereas vessels in the exocrine tissue were unchanged. The dilation of intraislet capillaries was independent of islet size, suggesting the vascular adaptation may primarily support increased β-cell insulin secretory demand rather than β-cell mass expansion. Moreover, these vascular changes were accompanied by an increase in islet parasympathetic innervation. Our results indicate that the metabolic state influences islet angioarchitecture and innervation, suggesting that islet neurovascular remodeling may influence whether β-cells can adequately respond to insulin resistance and maintain normoglycemia.

RESEARCH DESIGN AND METHODS

Animals. Animal studies were performed in accordance with guidelines of the Vanderbilt University Institutional Animal Care and Use Committee. Adult male and female *ob/wt* mice on the C57BL/6J background were bred and genotyped according to protocol provided by The Jackson Laboratory (Bar Harbor, ME). The *ob/ob* and *wt/wt* controls were studied at 4, 8, and 16 weeks of age. GLUT4$^{+/-}$ mice and their GLUT4$^{+/+}$ littermates were 48–50 weeks of age on mixed C57BL/6J/129 Sv/Black Swiss background, as previously described (12). For an insulin-resistant model of diet-induced obesity, male C57BL/6J mice (The Jackson Laboratory) were fed chow or a high-fat diet (HFD) starting at weaning until 20 weeks of age. The standard chow (LabDiet, cat. #5001) contained 48.7% carbohydrate, 23.9% protein, and 5.0% fat by weight with a total of 13.5% of dietary calories from fat. The HFD (Bio-Serv, Frenchtown, NJ, cat. #F3282) contained 36.3% carbohydrate, 20% protein, and 35.5% fat by weight with a total of 60% of dietary calories from fat. Food was changed twice weekly. Blood glucose and plasma insulin levels were measured in the fed and fasted state, as described (6).

From the [1]Division of Diabetes, Endocrinology, and Metabolism, Department of Medicine, Vanderbilt University Medical Center, Nashville, Tennessee; the [2]Department of Surgery, Vanderbilt University Medical Center, Nashville, Tennessee; the [3]Department of Molecular Physiology and Biophysics, Vanderbilt University Medical Center, Nashville, Tennessee; the [4]Division of Nephrology and Hypertension, Department of Medicine, Vanderbilt University Medical Center, Nashville, Tennessee; and the [5]Veterans Affairs Tennessee Valley Healthcare System, Nashville, Tennessee.

Corresponding author: Alvin C. Powers, al.powers@vanderbilt.edu.

Received 30 November 2012 and accepted 17 April 2013.

DOI: 10.2337/db12-1657

This article contains Supplementary Data online at http://diabetes.diabetesjournals.org/lookup/suppl/doi:10.2337/db12-1657/-/DC1.

C.D. and M.B. contributed equally to this work.

See accompanying articles, pp. 4004, 4154, and 4165.

Quantitative RT-PCR. Total islet RNA was extracted using an RNAqueous RNA isolation kit (Ambion, Austin, TX), and analysis was performed as described (13). TaqMan primers and probes were from Applied Biosystems (Supplementary Table 1).

Histological assessment of pancreas. Immunohistochemistry, morphometric analysis, and assessment of the functional islet vasculature were performed as described (6). Antigens were visualized with the primary antibodies listed in Supplementary Table 2. Secondary antibodies were from Jackson ImmunoResearch Laboratories, Inc. (West Grove, PA).

Blood flow imaging in vivo. Islet capillaries were visualized after a bolus of sulforhodamine-conjugated dextran, and islet blood flow was measured by tracking sulforhodamine-labeled erythrocytes (RBCs), as previously described (14). Internal islet capillary diameter was measured using Imaris 7.5 software (Bitplane, South Windsor, CT) on 20 capillaries in *wt/wt* and *ob/ob* mice ($n = 3$ islets/group).

Nitric oxide activity. Wild-type and *ob/ob* mice were perfused through cardiac puncture at a 1 mL/min flow rate with warm PBS for 5 min, followed by 10 mmol/L 4,5-diaminofluorescein diacetate (DAF-2DA; Alexis Biochemicals, Farmingdale, NY) containing 0.1 mmol/L L-arginine and 2 mmol/L $CaCl_2$ for 10 min, and a 10-min washout period with PBS (15). Production of nitric oxide (NO) converts the nonfluorescent dye, DAF-2 DA, to its fluorescent triazole derivative DAF-2T. Pancreata were removed and fixed, and cryosections were imaged, as described above. DAF-2T fluorescence intensity was measured using ImageJ software, and data were reported after background signal subtraction. Islets were deemed DAF-2T$^+$ only if DAF-2T fluorescence intensity was twofold higher compared with background.

Electron microscopy. Ultrastructure of β-cells and islet vasculature were assessed by transmission electron microscopy (6). Basement membrane thickness was measured in calibrated images at original magnification ×8,800–15,000 using ImageScope software (Aperio, Vista, CA). Depending on the capillary size, the basement thickness was measured at 10–15 points along the capillary length and then averaged per each capillary.

Statistical analysis. The Student t test was used for comparisons of two groups. All data are presented as mean ± SEM, and a P value < 0.05 was considered significant.

RESULTS

Characteristics of three mouse models of insulin resistance used for islet blood vessel analysis. To investigate if islet vascularization changes in the setting of insulin resistance, we studied three mouse models with different mechanisms of insulin resistance: *1*) *ob/ob* mice with an inactivating mutation in the leptin gene (16,17), *2*) mice heterozygous for inactivation of the GLUT4 glucose transporter gene (GLUT4$^{+/-}$) (12,18), and *3*) mice fed an HFD. The *ob/ob* and HFD mice were both obese relative to their respective controls, but GLUT4$^{+/-}$ mice had the same body weight as GLUT4$^{+/+}$ littermates (Supplementary Fig. 1*A–C*). When fasting plasma insulin was used as a measure of insulin resistance, *ob/ob* mice and HFD mice were more insulin-resistant than GLUT4$^{+/-}$ mice (Supplementary Fig. 1*E–G*). Fasting and random blood glucose levels in *ob/ob* mice were moderately elevated at 4, 8, and 16 weeks of age, and they were noted to be glucose-intolerant by 4 weeks of age (Supplementary Fig. 2*A* and *B*). HFD and GLUT4$^{+/-}$ mice had blood glucose levels similar to those of controls (Supplementary Fig. 2*C* and *D*). Islet size was significantly increased in all three insulin-resistant models but more profoundly in *ob/ob* and GLUT4$^{+/-}$ mice compared with HFD mice (Supplementary Fig. 1*H–P*).

Changes in islet angioarchitecture associated with insulin resistance. We reasoned that hyperplastic islets, like tumors, would need increased vascularization because of the increased β-cell number and increased metabolic demands associated with increased insulin biosynthesis and secretion. To assess the pancreatic islet vasculature, blood vessels were visualized by the intravital labeling with lectin-fluorescein isothiocyanate (FITC) (6) (Fig. 1*A–F*) or by using live imaging in vivo with a bolus of rhodamine-conjugated dextran (14) (Fig. 1*G* and *H*). These two methodologies take advantage of intravascular labeling that visualizes only functional vessels, and when combined with optical sectioning, allow for three-dimensional reconstruction of the islet angioarchitecture (Fig. 1*A–H*). This three-dimensional reconstruction revealed that capillaries in *ob/ob* islets were greatly enlarged as early as 4 weeks of age. The vessel enlargement was quite prominent within the islet core composed mainly of β-cells but was not observed in the islet periphery containing mainly non–β-cells (Fig. 1*D–F* and *H* and Supplementary Fig. 1*H–M*). Surprisingly, enlarged capillaries were detected not only in hyperplastic islets but also in medium and smaller size islets (Fig. 1*D*), suggesting that the capillary enlargement is independent of β-cell number per islet.

To better understand vascular phenotype in *ob/ob* islets, we used integrated morphometry to measure several vessel parameters using 10-μm-thick cryosections labeled with lectin-FITC. At 1 week of age, *ob/ob* mice were insulin-resistant (Supplementary Fig. 1*D*), but islet vascular parameters were similar to *wt/wt* mice (Fig. 1*I–K*). Although overall blood vessel area-to-islet area ratio increased in *ob/ob* compared with *wt/wt* islets by 4 weeks of age (Fig. 1*I*), islet vascular density progressively declined in *ob/ob* mice with age (Fig. 1*J*). At the same time, intraislet vessels became larger in *ob/ob* mice, as reflected by an 81% increase in the area/vessel parameter (Fig. 1*K*). This was further confirmed by measurement of the internal capillary diameter demonstrating that capillaries in *ob/ob* mice were more than twofold thicker (Fig. 1*N*). In contrast to islets, the vasculature of exocrine tissue was unchanged in insulin-resistant *ob/ob* mice (Fig. 1*M* and *N*). In addition, lectin-FITC labeling in the islets and exocrine tissue was colocalized with EC markers such as caveolin-1 and CD31, confirming that blood vessels in both pancreatic compartments were quiescent and not forming new sprouts (data not shown) (6,19). These data indicate that insulin resistance in the *ob/ob* model leads to increased vessel area per islet. However, this increase in islet vascular supply results not from increasing islet vessel density but, rather, from capillary size.

Because *ob/ob* mice have a number of metabolic changes and the leptin receptor is expressed in ECs (20), we examined islet vascularization in two additional models of insulin resistance: one associated with obesity (HFD mice) and the other one without obesity (GLUT4$^{+/-}$ mice). Using EC labeling with caveolin-1, we found that islet vasculature in these two models (Fig. 2) was phenotypically similar to that of *ob/ob* islets (Fig. 1). The vessel area-to-islet area ratio was increased in HFD and GLUT4$^{+/-}$ mice compared with their respective controls (Fig. 2*C* and *H*) and accompanied by reduced vessel density (Fig. 2*D* and *I*) and a 51–80% increase in the area-to-vessel ratio (Fig. 2*E* and *J*), demonstrating intraislet capillary enlargement. These results demonstrate that increasing islet vascular supply through islet capillary enlargement is a common adaptive response to insulin resistance.

Insulin resistance does not lead to islet angiogenesis. Tissue vascular development and adult blood vessel homeostasis are coordinated through intricate signaling networks of several angiogenic growth factor families (3,4,21,22). Islet endocrine cells express several angiogenic factors, but VEGF-A is a principal regulator of islet capillary density and vascular permeability (5,6). Because insulin resistance led to an increased ratio of blood vessel area to islet area, we asked if this increase in islet vascular

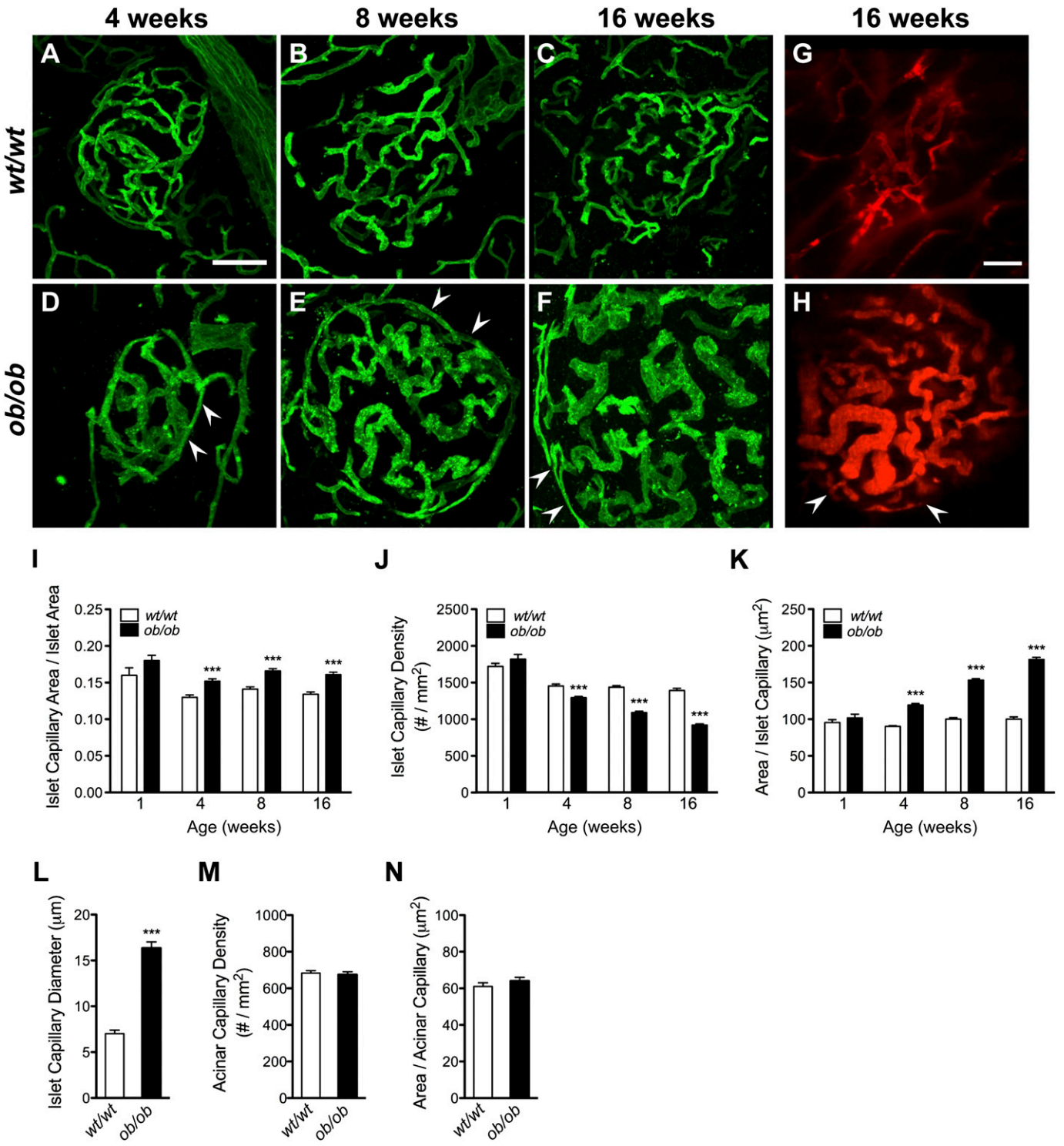

FIG. 1. Reduced islet vessel density but increased vessel size in insulin-resistant *ob/ob* mice. *A–F*: Islet vasculature in *wt/wt* and *ob/ob* mouse pancreas was visualized by intravital labeling with FITC-conjugated endothelium-binding tomato lectin. Pancreatic sections (60 μm) were optically sectioned, and islet vasculature was three-dimensionally reconstructed. The scale bar in *A* represents 50 μm and applies to *B–F*. *G* and *H*: Three-dimensional projections of islet capillaries visualized after a bolus of rhodamine-conjugated dextran by live imaging in vivo. The arrowheads in *D–H* point to capillaries in the islet periphery. The scale bar in *G* represents 50 μm and applies to *H*. Images in *A–H* are representative three-dimensional projections of islet capillaries obtained from 3 *ob/ob* mice and 3 *wt/wt* controls at 16 weeks of age with 3–5 islets/mouse. *I–K*: Vascular morphometry was performed on 10-μm cryosections, with blood vessels visualized by intravital labeling with lectin-FITC (6,19). MetaMorph 6.1 software (Universal Imaging) was used to apply integrated morphometry analysis to at least 40 islets per tissue block or comparable areas of acinar tissue (n = 4–5 mice/genotype) to determine ratio of islet capillary area to islet area, capillary density, and area per capillary. Capillaries were counted using a technique described by Weidner (49), where any fluorescently labeled EC or EC cluster clearly separate from adjacent microvessels was considered a single, countable microvessel. *L*: Islet capillary diameter was measured on 20 capillaries visualized by a bolus of sulforhodamine-conjugated dextran in *wt/wt* and *ob/ob* mice at 16 weeks of age (n = 3 islets/group). Capillary density (*M*) and area per capillary (*N*) in acinar tissue were not statistically different in *wt/wt* and *ob/ob* mice at 8 weeks of age (at least 40 acinar tissue areas were analyzed per mouse; n = 4 mice/genotype). ***$P < 0.001$ *ob/ob* compared with *wt/wt*.

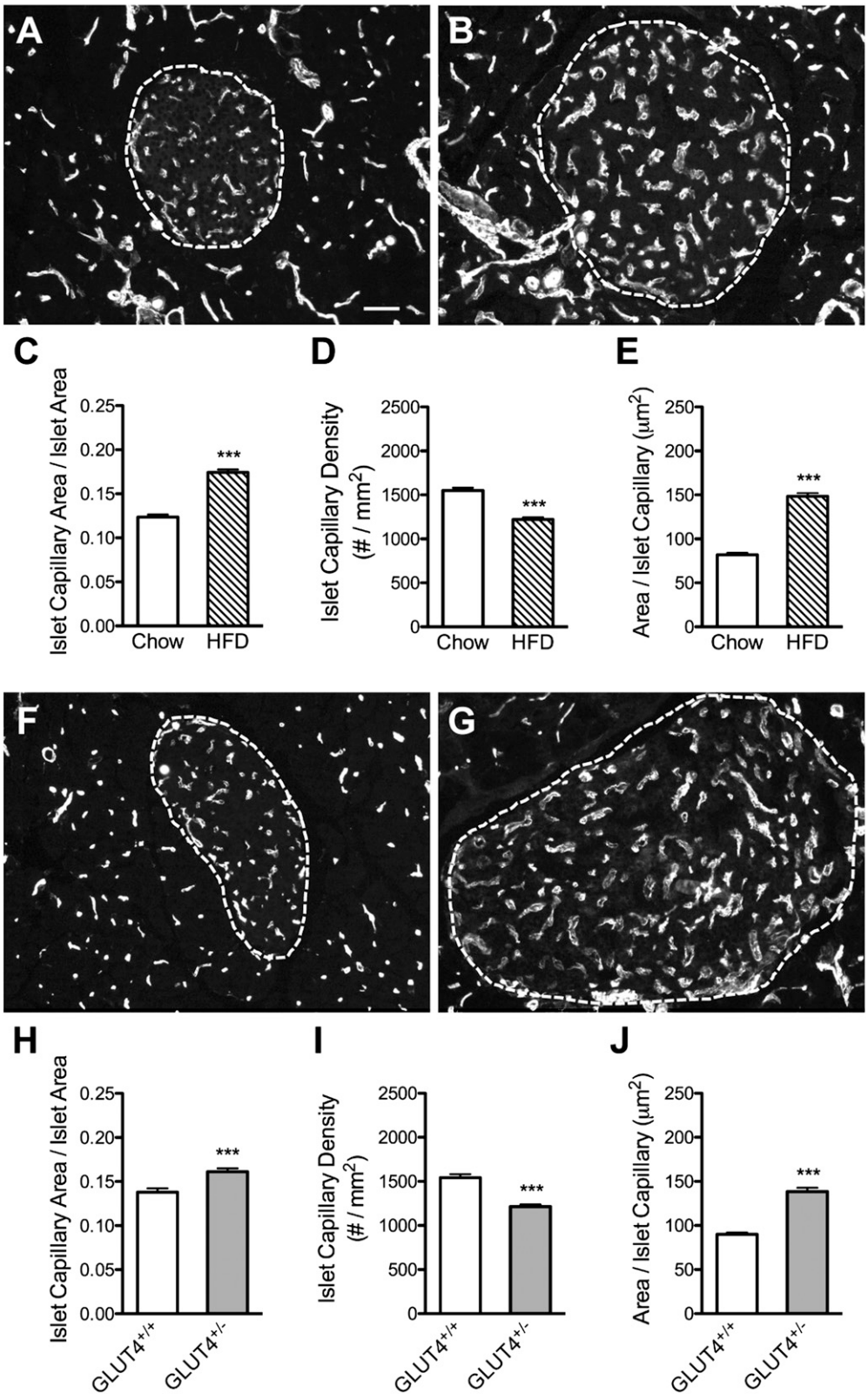

FIG. 2. Reduced islet vessel density and increased vessel area in mice with insulin resistance due to HFD or GLUT4 heterozygosity. Islet vasculature in C56BL/6 mice fed chow (*A*) or HFD (*B*) visualized by EC labeling with caveolin-1. *C–E*: Morphometric analysis of islet vasculature in mice fed chow or HFD. Islet vasculature in GLUT4$^{+/+}$ (*F*) and GLUT4$^{+/-}$ (*G*) was visualized by EC labeling with caveolin-1. *H–J*: Morphometric analysis of islet vasculature in GLUT4$^{+/+}$ and GLUT4$^{+/-}$ mice. The scale bar in *A* represents 50 μm and applies to *B*, *F*, and *G*. ***$P < 0.001$ HFD or GLUT4$^{+/-}$ mice compared with respective controls (n = 4–5 mice and >100 islets/genotype).

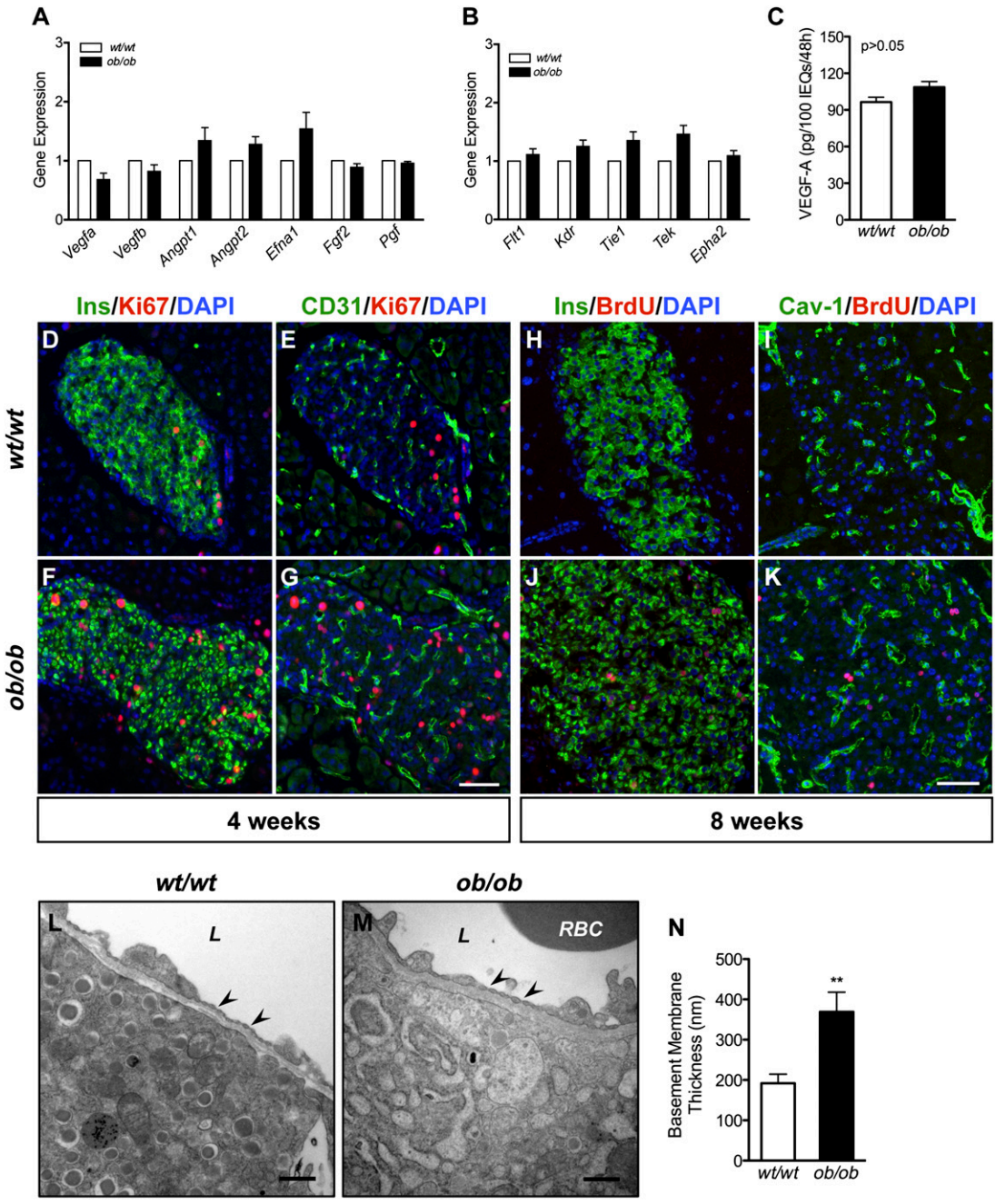

FIG. 3. Islet angiogenic factor expression and EC fenestrations are not altered in insulin resistance. Gene expression profile of angiogenic factors (*A*) and their receptors (*B*) in *wt/wt* and *ob/ob* islets at 8 weeks of age was measured by quantitative RT-PCR. Gene expression analysis was performed on islets isolated from five separate mice per genotype ($P > 0.05$). Quantitative RT-PCR data were normalized to endogenous *B2m* control and then expressed relative to *wt/wt* control. *Ins1* mRNA level was not different in *ob/ob* and *wt/wt* islets, and *Ins2* mRNA level was modestly increased in *ob/ob* islets (40 ± 10% increase in *ob/ob* compared with *wt/wt*). *C*: VEGF-A secretion in isolated size-matched *wt/wt* ($n = 5$ samples) and *ob/ob* islets ($n = 4$ samples) was assessed as described previously (6) and normalized per 100 islet equivalents (IEQs) (50). Pancreatic sections from *wt/wt* (*D* and *E*) and *ob/ob* (*F* and *G*) mice at 4 weeks of age were stained for insulin (Ins, green), Ki67 (red), and CD31 (green) and counterstained with DAPI (blue). No Ki67$^+$/CD31$^+$ ECs were detected in *wt/wt* or *ob/ob* pancreatic sections. The scale bar in *G* represents 50 μm and applies to *D–F*. Pancreatic sections from *wt/wt* (*H* and *I*) and *ob/ob* (*J* and *K*) mice at 8 weeks of age were stained for insulin (Ins, green), BrdU (red), and caveolin-1 (Cav-1, green) and counterstained with DAPI (blue). No BrdU$^+$/caveolin-1$^+$ ECs were detected in *wt/wt* or *ob/ob* pancreatic sections. BrdU (Sigma-Aldrich) was administered in drinking water at 0.8 mg/mL for 7 days before tissue collection. The scale bar in *K* represents 50 μm and applies to *H–J*. EC ultrastructure of islet vasculature in *wt/wt* (*L*) and *ob/ob* (*M*) was assessed by transmission electron microscopy. The arrowheads point to EC fenestrations; *L*, capillary lumen; *RBC*, red blood cell. The scale bar in *L* and *M* represents 500 nm. *N*: Basement membrane thickness in *wt/wt* and *ob/ob* was analyzed by transmission electron microscopy and morphometry ($n = 10$ capillaries/genotype, $n = 2$ mice/genotype). $^{**}P < 0.01$.

supply was modulated by changes in islet angiogenic growth factor expression. To address this question, we investigated the expression profile of several angiogenic growth factor families, including VEGFs, angiopoietins, fibroblast growth factors, and ephrins, by quantitative RT-PCR in control and *ob/ob* islets. As expected, mRNA levels of *Vegfa* and its obligatory receptors *Flt1* and *Kdr* were the most abundant among all of the angiogenic factors and receptors examined (data not shown). None of the angiogenic factors or their receptors were differentially

expressed in *ob/ob* versus control islets (Fig. 3*A* and *B*), suggesting that islet vascular expansion associated with insulin resistance is not mediated by angiogenesis. A caveat of this analysis is that *ob/ob* islets may have fewer ECs per islet volume due to the increased β-cell population, and thus, angiogenic factor receptor mRNA could be unchanged due to the increased number of receptors on intraislet ECs. Consistent with the gene expression analysis in Fig. 3*A*, VEGF-A production was similar in *wt/wt* and *ob/ob* islets (Fig. 3*C*).

To further confirm that intraislet EC proliferation was not contributing to islet vascular changes, we assessed replication in *ob/ob* and *wt/wt* mice at 4 and 8 weeks of age. Although proliferating β-cells were abundant in *ob/ob* islets compared with controls (Fig. 3*D*, *F*, *H*, and *J*), we did not detect intraislet EC proliferation in either type of islets (Fig. 3*E*, *G*, *I*, and *K*). These data, together with those in Fig. 3*A–C*, indicate that islet angiogenesis during insulin resistance is very rare, with islet vasculature characterized by a relative stability and a very low mitotic activity of the intraislet EC population. Furthermore, these data suggest that even if the number of VEGF receptor 1 (encoded by *Flt1*) and VEGF receptor 2 (encoded by *Kdr*) receptors increased on intraislet ECs in *ob/ob* islets, this increase did not have an important biological effect.

In addition, transmission electron microscopy demonstrated that intraislet ECs in *ob/ob* islets had an abundance of fenestrations similar to that in control islets (Fig. 3*L* and *M*). Although the basement membrane thickness increased nearly twofold in *ob/ob* islets (Fig. 3*N*), this increase represents less than 1% of the islet vessel diameter (Fig. 1*L*). Taken together, our results show that islet vascular expansion associated with insulin resistance is not mediated by angiogenesis. Instead, adaptive changes in islet vasculature result from dilation of preexisting vessels.

Mechanisms of intraislet vessel dilation in response to insulin resistance. To dissect the mechanisms of the islet blood vessel dilation, we first examined islet capillary support structures. In islets, this capillary support is provided mainly by endocrine cells and pericytes. Hellström at al. (23) showed previously that the lack of pericytes leads to EC hyperplasia, vessel dilation, and microaneurysm formation. Transmission electron microscopy revealed RBC extravasation indicative of intraislet hemorrhage formation, especially in large islets of *ob/ob* mice at 16 weeks of age (Supplementary Fig. 3). To assess the status of pericytes in *ob/ob* islets, pancreatic sections were labeled for two pericyte markers: NG2 and platelet-derived growth factor receptor β (PDGFRβ). We found that pericytes were present in *ob/ob* islets and as demonstrated by immunolabeling, and their area appeared to be increased compared with *wt/wt* islets (Fig. 4*A–F*). The ultrastructural analysis further demonstrated that pericytes around the intraislet capillaries were hypertrophied in *ob/ob* islets

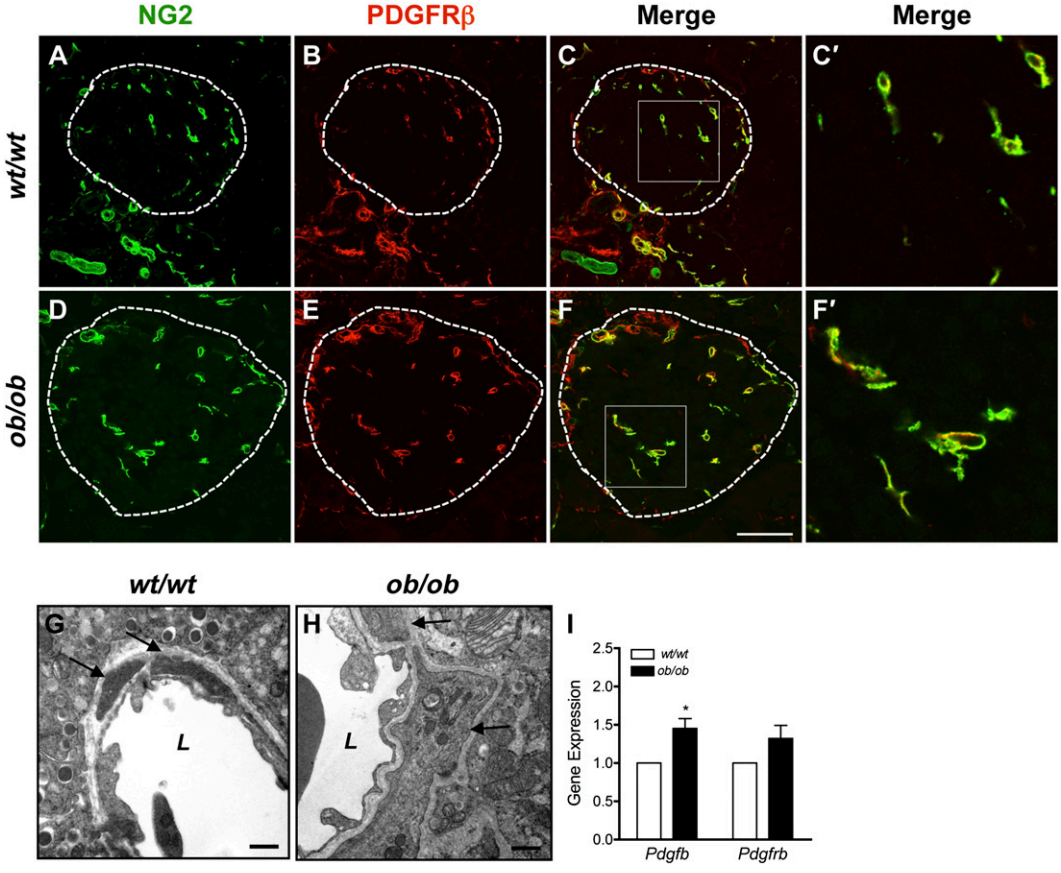

FIG. 4. Pericytes associated with intraislet capillaries become hypertrophied during insulin resistance. Pancreatic sections from *wt/wt* (*A–C*) and *ob/ob* mice (*D–F*) at 16 weeks of age were colabeled with the pericyte markers NG2 (green) and PDGFRβ (red). The dashed line denotes the islet perimeter. The boxes in *C* and *F* denote enlargements in *C′* and *F′*. The scale bar in *F* represents 50 μm and also applies to *A–E*. Transmission electron microscopy micrographs of *wt/wt* (*G*) and *ob/ob* islet (*H*). The arrows point to normal pericytes in *G* and to hypertrophied pericytes in *H*; *L*, capillary lumen. The scale bar in *G* and *H* represents 500 nm. *I*: *Pdgfb* and *Pdgfrb* mRNA expression was determined by quantitative RT-PCR. Gene expression analysis was performed on islets isolated from four separate mice per genotype. Quantitative RT-PCR data were normalized to endogenous *B2m* control and then expressed relative to *wt/wt*. *$P < 0.05$.

(Fig. 4*G* and *H*). This pericyte hypertrophy was associated with increased expression of the *Pdgfb*/*Pdgfrb* ligand-receptor system in *ob*/*ob* islets (Fig. 4*I*).

Nervous system input plays an important role in the regulation of islet blood flow to maintain homeostasis and react to normal fluctuations in metabolic demands (24,25). To determine if nervous system changes occur in chronic islet adaptation to insulin resistance, we examined the morphology of islet autonomic innervation. Global islet innervation was increased in hyperplastic *ob*/*ob* islets (Fig. 5*A* and *B*), as quantified by the density of nerve fibers labeled for neuronal class III β-tubulin, the neuron-specific tubulin marker (Fig. 5*E*). Islets in *ob*/*ob* mice also showed dense parasympathetic innervation, with numerous nerve fibers expressing the vesicular acetylcholine transporter (VAChT) (Fig. 5*C* and *D*). When quantified, the density of VAChT$^+$ varicosities and the VAChT$^+$ area were both increased in *ob*/*ob* islets (Fig. 5*F* and *G*). The change was not due to larger islets in *ob*/*ob* mice, because the similarly sized islets in *wt*/*wt* mice did not show the same increase in VAChT$^+$ nerve fibers (Supplementary Fig. 4*A* and *B*). In contrast to parasympathetic innervation, islet sympathetic innervation was unchanged in *ob*/*ob* mice, as evaluated by staining for tyrosine hydroxylase (TH), the rate-limiting enzyme in catecholamine biosynthesis. Islets from *ob*/*ob* and *wt*/*wt* mice showed a comparable number of TH$^+$ nerve fibers within the insulin$^+$ islet core (Supplementary Fig. 4*C* and *D*). Similarly, *ob*/*ob* and *wt*/*wt* mice both showed a few TH$^+$ β-cells per islet (Supplementary Fig 4*C* and *D*). These data demonstrate that *ob*/*ob* islets have enhanced parasympathetic innervation that may contribute to increased blood flow in *ob*/*ob* islets.

To measure islet blood flow, we used live imaging and tracked sulforhodamine-labeled RBCs in vivo (14). We used the RBC trajectory to calculate RBC speed and found that it was 30% higher in *ob*/*ob* islets (Fig. 5*H*). Carlsson et al. (26) found that *ob*/*ob* mice had a major increase in islet blood (fourfold) at 4 weeks of age. Our longitudinal analysis of islet capillary morphometry (Fig. 1*K*) complements the islet blood flow data by Carlsson et al. (26), indicating that the robust increase in islet blood flow at 4 weeks of age precedes adaptive changes in the islet capillary size. This suggests that islet capillary diameter responds to increased islet blood flow and that shear stress leads at least in part to islet capillary dilation.

Increased blood flow and shear stress induce transcription and translation of endothelial NO synthase (eNOS), which leads to increased synthesis and release of the potent vasodilator, NO (27). All three isoforms of NOS are present in *wt*/*wt* islets, but the mRNA level of eNOS (*Nos3*) was higher than neuronal NOS (*Nos1*) and inducible NOS (*Nos2*) (Fig. 6*A*). Moreover, *ob*/*ob* islets had higher expression of *Nos3* but lower expression of *Nos1* and *Nos2* (Fig. 6*B*). We next measured NO production in vivo using the fluorescent NO indicator DAF-2DA. In *ob*/*ob* islets, DAF-2T fluorescence intensity increased by 30% (Fig. 6*C*–*G*), although some *wt*/*wt* and *ob*/*ob* islets had similar DAF-2T fluorescence intensity. These data indicate that islet

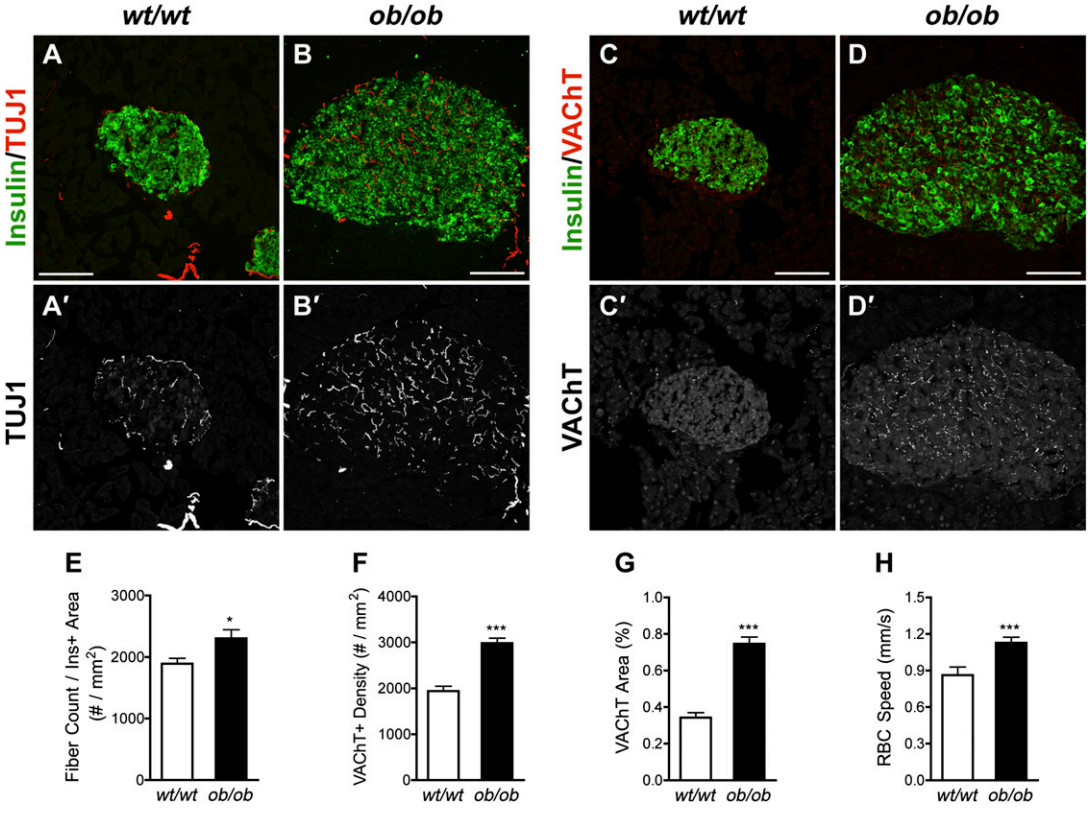

FIG. 5. Enhanced parasympathetic innervation and blood flow in *ob*/*ob* islets. Islets from *ob*/*ob* mice (*B* and *D*) and their *wt*/*wt* controls (*A* and *C*) were immunolabeled for insulin (green) and neuronal class III β-tubulin (TUJ1; red/grayscale in *A′* and *B′*) or VAChT (red/grayscale in *C′* and *D′*). The scale bars are 100 μm. *E*–*G*: Global islet innervation density was quantified by calculating the number of TUJ1$^+$ fibers within the insulin$^+$ islet area. Islet parasympathetic innervation was quantified by calculating the number of VAChT$^+$ varicosities per insulin$^+$ area and by calculating the VAChT$^+$ area as a percentage of the insulin$^+$ islet area. Quantification is shown for islet TUJ1$^+$ nerve fiber density (*E*), islet VAChT$^+$ varicosity density (*F*), and islet VAChT$^+$ area (*G*) (*n* = 100 islets/genotype). *H*: Islet blood flow was measured by tracking sulforhodamine-labeled RBCs in *wt*/*wt* and *ob*/*ob* mice at 16 weeks of age (*n* = 90/genotype). Ins$^+$, insulin$^+$. *$P < 0.05$ and ***$P < 0.001$ *ob*/*ob* compared with *wt*/*wt*.

vascular changes during insulin resistance are closely associated with increased islet parasympathetic innervation and islet blood flow and are at least partly mediated by increased NO production.

DISCUSSION

Pancreatic islets respond to the increased insulin demand associated with insulin resistance by increasing insulin output and expanding β-cell mass. These compensatory changes are critical for maintaining normoglycemia and avoiding diabetes. Because islets are highly vascularized and many of the adaptive changes in islets are accompanied by increased oxygen and nutrient requirements, we assessed islet vascularization in three independent mouse models of insulin resistance: leptin deficiency, HFD-induced obesity, and GLUT4 haploinsufficiency. Our results indicate that the islet vascular supply increases during insulin resistance. However, this vascular adaptation is mediated not by angiogenesis but, rather, by dilation of preexisting vessels.

Despite the dramatic changes in β-cell mass and function during insulin resistance, islets, unlike tumors, surprisingly maintain normal expression of the major angiogenic factor secreted by islet endocrine cells, *Vegfa*, and its signaling receptors *Kdr* and *Flt1*. Several recent reports indicate that the precise regulation of VEGF-A signaling is critical for the maintenance of vascular homeostasis in developing and mature islets (28–30), and our data suggest that this tight regulation of VEGF-A signaling is conserved even in insulin resistance. Increased VEGF-A expression by endocrine progenitors or β-cells stimulates proliferative angiogenesis that leads to β-cell loss (28,29). Although islets in insulin-resistant animals showed increased β-cell proliferation, there was no proliferation of intraislet ECs, indicating that islet vasculature is quiescent. Prior studies using prediabetic Zucker diabetic fatty rats and HFD-fed mice suggested a causal relationship between increased islet VEGF-A secretion and islet hypervascularization in insulin resistance, but these studies did not normalize islet VEGF-A production for the difference in the total cell number between hyperplastic and control islets (30,31). Our data show that these studies overestimated VEGF-A production per islet and that this is the reason for the difference with our results. Furthermore, because the number of islet capillaries is strictly regulated by VEGF-A (5,6), the fact that islets compensate by increasing the vessel size and not by changing the vessel number, EC proliferation, or EC fenestration is biologic evidence of VEGF-A–independent vascular adaptation. Formation of larger vessels was noted when Ang-1 was overexpressed in the skin (32), but our analysis suggests that the angiopoietin signaling system is not involved in the increased islet capillary size associated with insulin resistance.

Islet capillaries not only increased in size but also underwent several changes at the ultrastructural level. Although EC fenestrations were maintained in the insulin-resistant

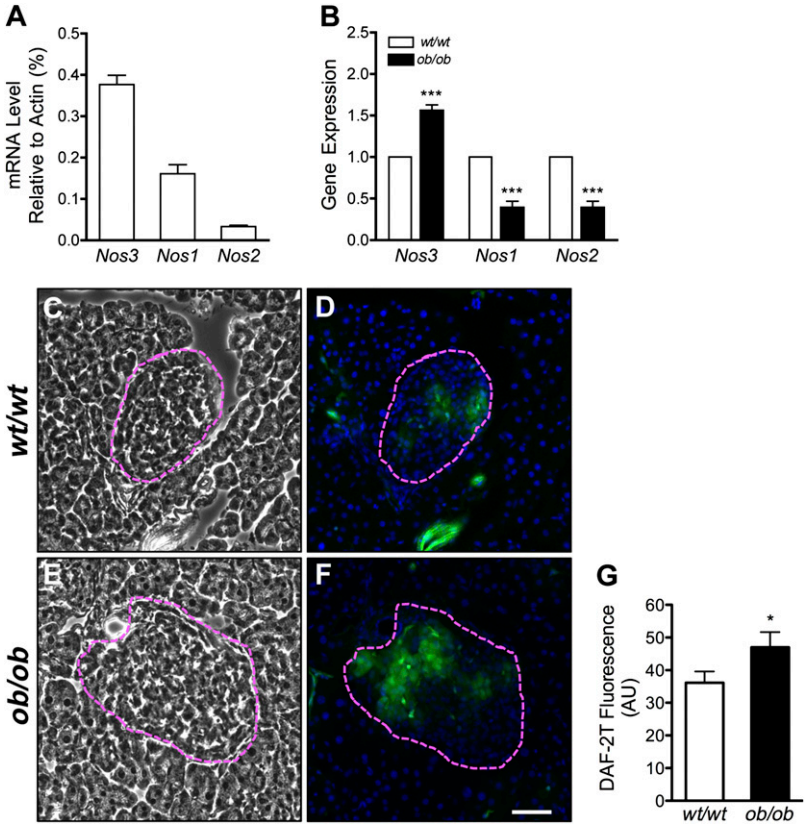

FIG. 6. Expression of NOS isoforms and NO production in *wt/wt* and *ob/ob* islets. *A*: The expression level of three NOS isoforms in *wt/wt* islets was measured by quantitative RT-PCR (n = 5 islet samples) and expressed relative to *Actb*. *B*: Expression profile of *Nos1*, *Nos2*, and *Nos3* in *wt/wt* and *ob/ob* islets at 8 weeks of age (n = 5 samples/genotype). *B2m* was used as an endogenous control in *A* and *B*. *C–G*: NO production in *wt/wt* and *ob/ob* islets was measured by DAF-2T fluorescence in vivo. Phase contrast images of pancreatic cryosections from *wt/wt* (*C*) and *ob/ob* mice (*E*), with islet boundaries denoted by the dashed line. *D* and *F*: DAF-2T fluorescence within islet boundaries marked in *C* and *E*. *G*: Intensity of DAF-2T fluorescence. AU, arbitrary unit. *P < 0.05; ***P < 0.001 *ob/ob* compared with *wt/wt*.

state, the thickness of the vascular basement membrane nearly doubled, the pericytes associated with islet capillaries became hypertrophied, and we noted RBC extravasation. Similar changes in basement membrane and pericytes were reported by Nakamura et al. (33) in islets of diabetic *db*/*db* mice. We showed that the thickness of the islet capillary basement membrane increased proportionally with the capillary diameter but did not observe hallmarks of fibrosis, such as presence of fibroblasts as reported by Nakamura et al. (33) in *db*/*db* mice with longstanding diabetes (34). Because the capillary basement membrane in islets is exclusively synthesized by intraislet ECs (35), its remodeling during insulin resistance could be caused by changes in ECs triggered by increased islet blood flow (36). Thus, the increased basement membrane thickness in the absence of diabetes could be viewed as an initial adaptive response of intraislet ECs rather than fibrosis, as proposed by Agudo et al. (30). Furthermore, Agudo et al. (30) suggested that the increased area of islet vascular collagen IV labeling during insulin resistance was indicative of fibrosis. Our data do not support this conclusion and instead indicate that the increased area of collagen IV, which marks blood vessel surface, is mainly due to the increased islet capillary size and not fibrosis.

The role of pericytes in normal islet function is not completely understood, but in other tissues, pericytes are very important in supporting blood vessel stability (23,37,38). ECs recruit pericytes to the vessel wall mainly by secreting PDGFB homodimer that binds to PDGFRβ receptor on the pericyte surface. Inactivation of PDGFB or PDGFRβ results in pericyte loss that leads to EC hyperplasia, vessel dilation, and vascular leakage (23,37,38). In the *ob*/*ob* model, pericytes were not lost, and actually, *Pdgfb*/*Pdgfrb* expression and pericyte area were slightly increased. We thus postulate that this compensation is insufficient in the presence of significantly increased islet vascular perfusion and leads to vessel instability and hemorrhaging. Our gene expression and vascular morphometry data strongly argue against the notion that the primary cause of vascular leakage in the insulin resistance setting is increased islet VEGF-A expression (30,31).

Our data indicate that insulin resistance leads to significantly increased expression of eNOS (*Nos3*), a rate-limiting enzyme in NO synthesis. NO plays a key role in regulating endothelium-dependent vasodilation (39). Several complementary mechanisms may lead to increased *Nos3* expression and NO production resulting in NO-mediated islet capillary dilation during insulin resistance. The NO-mediated vasodilatory response of intraislet ECs may be stimulated by hemodynamic shear stresses imposed on endothelium by higher islet blood flow. ECs respond to changes in blood flow through the process known as mechanotransduction (27,36). We propose that this response increases expression of eNOS and thus results in greater availability of NO.

We also observed that islets during insulin resistance have increased parasympathetic innervation, while maintaining normal sympathetic innervation. Islet parasympathetic nerves release neurotransmitters such as ACh, vasoactive intestinal peptide, gastrin-releasing peptide, and pituitary adenylate cyclase-activating polypeptide and play critical roles in regulating hormone release and in determining blood vessel tone (40–43). When glucose is infused specifically in the brain, signals from the central nervous system are transmitted through the vagus nerves to enhance insulin secretion and islet blood flow (25). In addition, glucose infusion directly into the duodenum triggers a vagal relay to induce similar

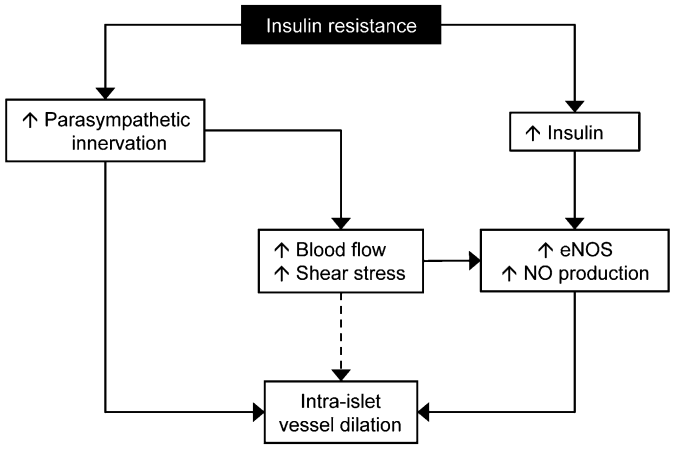

FIG. 7. Proposed model of mechanisms leading to islet vascular changes in insulin-resistant mice. Details are outlined in the DISCUSSION.

effect (24). The increased density of cholinergic nerves that we observed in *ob*/*ob* islets supports the importance of the parasympathetic nervous system in mediating the increased insulin secretion and islet blood flow in obese mice and rats (44–46). For example, ACh activates muscarinic receptors on ECs, which results in the release of NO leading to relaxation of vascular smooth muscle cells and vasodilation (47). Further studies are required to understand the mechanisms regulating islet parasympathetic innervation during insulin resistance and the relationship between parasympathetic innervation and adaptive changes in islet vascularization.

Our three-dimensional reconstruction of islet capillaries demonstrated that the dilation was present only in the islet core containing mostly β-cells and not around the periphery composed of other islet hormone-producing cell types. This unique arrangement of islet angioarchitecture suggests that β-cells may be involved in islet capillary dilation. Because insulin secretion is markedly increased during insulin resistance, it is possible that the local increase in insulin levels activates the insulin receptor signaling cascade in intraislet ECs leading to phosphatidyl inositol 3-kinase-Akt-mediated eNOS activation, increased NO production, and vasorelaxation (48).

Here we show that the pancreatic islet adaptation to insulin resistance is not limited to changes within β-cells but also involves islet-specific, neurovascular remodeling. To accommodate the increased demand for insulin delivery into the peripheral circulation, islet capillaries expand by dilation and not by angiogenesis. Based on our data, we propose a model where eNOS-dependent islet capillary dilation is modulated by complementary signals derived from β-cells, parasympathetic nerves, and islet blood flow (Fig. 7). In addition, islet capillary dilation is accompanied by basement membrane remodeling and pericyte hypertrophy. These changes in the structural support of islet capillaries may be insufficient to maintain capillary function, resulting in microaneurysm and β-cell damage. The adaptive changes in islet vascularization may influence the ability of islets to respond to insulin resistance and could be vital for preventing β-cell failure and development of type 2 diabetes.

ACKNOWLEDGMENTS

This work was supported by a Merit Review Award from the Veterans Affairs Research Service (BX000666); by National

Institutes of Health (NIH) grants DK-69603, DK-68764, DK-089572, DK-66636, DK-63439, and DK-072473; and by grants from JDRF, the Vanderbilt Mouse Metabolic Phenotyping Center (NIH Grant DK-59637), and the Vanderbilt Diabetes Research and Training Center (Islet Procurement and Analysis Core, NIH Grant DK-20593). Imaging was performed with support from the Vanderbilt University Medical Center Cell Imaging Shared Resource (NIH grants CA-68485, DK-20593, DK-58404, HD-15052, DK-59637, and EY-08126).

No potential conflicts of interest relevant to this article were reported.

C.D., M.B., R.B.R., L.N., M.S., T.T., and A.C.P. researched data and designed experiments. C.D., M.B., R.B.R., L.N., C.T., and A.S. performed experiments and reviewed data. E.H.L. reviewed data. C.D., M.B., R.B.R., E.H.L., and A.C.P. wrote the manuscript. C.D., M.B., R.B.R., L.N., E.H.L., C.T., A.S., M.S., T.T., and A.C.P. reviewed the manuscript. A.C.P. is the guarantor of this work and, as such, had full access to all the data in the study and takes responsibility for the integrity of the data and the accuracy of the data analysis.

Parts of this study were presented in abstract form at the 69th Scientific Sessions of the American Diabetes Association, New Orleans, Louisiana, 5–9 June 2009.

REFERENCES

1. Lifson N, Lassa CV, Dixit PK. Relation between blood flow and morphology in islet organ of rat pancreas. Am J Physiol 1985;249:E43–E48
2. Murakami T, Miyake T, Tsubouchi M, Tsubouchi Y, Ohtsuka A, Fujita T. Blood flow patterns in the rat pancreas: a simulative demonstration by injection replication and scanning electron microscopy. Microsc Res Tech 1997;37:497–508
3. Adams RH, Alitalo K. Molecular regulation of angiogenesis and lymphangiogenesis. Nat Rev Mol Cell Biol 2007;8:464–478
4. Augustin HG, Koh GY, Thurston G, Alitalo K. Control of vascular morphogenesis and homeostasis through the angiopoietin-Tie system. Nat Rev Mol Cell Biol 2009;10:165–177
5. Lammert E, Gu G, McLaughlin M, et al. Role of VEGF-A in vascularization of pancreatic islets. Curr Biol 2003;13:1070–1074
6. Brissova M, Shostak A, Shiota M, et al. Pancreatic islet production of vascular endothelial growth factor—a is essential for islet vascularization, revascularization, and function. Diabetes 2006;55:2974–2985
7. Lammert E, Cleaver O, Melton D. Induction of pancreatic differentiation by signals from blood vessels. Science 2001;294:564–567
8. Yoshitomi H, Zaret KS. Endothelial cell interactions initiate dorsal pancreas development by selectively inducing the transcription factor Ptf1a. Development 2004;131:807–817
9. Wang Q, Jin T. The role of insulin signaling in the development of β-cell dysfunction and diabetes. Islets 2009;1:95–101
10. Talchai C, Lin HV, Kitamura T, Accili D. Genetic and biochemical pathways of beta-cell failure in type 2 diabetes. Diabetes Obes Metab 2009;11(Suppl. 4):38–45
11. Chung AS, Lee J, Ferrara N. Targeting the tumour vasculature: insights from physiological angiogenesis. Nat Rev Cancer 2010;10:505–514
12. Brissova M, Blaha M, Spear C, et al. Reduced PDX-1 expression impairs islet response to insulin resistance and worsens glucose homeostasis. Am J Physiol Endocrinol Metab 2005;288:E707–E714
13. Dai C, Brissova M, Hang Y, et al. Islet-enriched gene expression and glucose-induced insulin secretion in human and mouse islets. Diabetologia 2012;55:707–718
14. Nyman LR, Ford E, Powers AC, Piston DW. Glucose-dependent blood flow dynamics in murine pancreatic islets in vivo. Am J Physiol Endocrinol Metab 2010;298:E807–E814
15. Kanetsuna Y, Takahashi K, Nagata M, et al. Deficiency of endothelial nitric-oxide synthase confers susceptibility to diabetic nephropathy in nephropathy-resistant inbred mice. Am J Pathol 2007;170:1473–1484
16. Zhang Y, Proenca R, Maffei M, Barone M, Leopold L, Friedman JM. Positional cloning of the mouse obese gene and its human homologue. Nature 1994;372:425–432
17. Bock T, Pakkenberg B, Buschard K. Increased islet volume but unchanged islet number in *ob/ob* mice. Diabetes 2003;52:1716–1722
18. Rossetti L, Stenbit AE, Chen W, et al. Peripheral but not hepatic insulin resistance in mice with one disrupted allele of the glucose transporter type 4 (GLUT4) gene. J Clin Invest 1997;100:1831–1839
19. McDonald DM, Choyke PL. Imaging of angiogenesis: from microscope to clinic. Nat Med 2003;9:713–725
20. Sierra-Honigmann MR, Nath AK, Murakami C, et al. Biological action of leptin as an angiogenic factor. Science 1998;281:1683–1686
21. Carmeliet P. Angiogenesis in health and disease. Nat Med 2003;9:653–660
22. Pasquale EB. Eph receptors and ephrins in cancer: bidirectional signalling and beyond. Nat Rev Cancer 2010;10:165–180
23. Hellström M, Gerhardt H, Kalén M, et al. Lack of pericytes leads to endothelial hyperplasia and abnormal vascular morphogenesis. J Cell Biol 2001;153:543–553
24. Carlsson P-O, Iwase M, Jansson L. Stimulation of intestinal glucoreceptors in rats increases pancreatic islet blood flow through vagal mechanisms. Am J Physiol 1999;276:R233–R236
25. Jansson L, Hellerström C. Glucose-induced changes in pancreatic islet blood flow mediated by central nervous system. Am J Physiol 1986;251:E644–E647
26. Carlsson P-O, Andersson A, Jansson L. Influence of age, hyperglycemia, leptin, and NPY on islet blood flow in obese-hyperglycemic mice. Am J Physiol 1998;275:E594–E601
27. Davies PF. Hemodynamic shear stress and the endothelium in cardiovascular pathophysiology. Nat Clin Pract Cardiovasc Med 2009;6:16–26
28. Sand FW, Hörnblad A, Johansson JK, et al. Growth-limiting role of endothelial cells in endoderm development. Dev Biol 2011;352:267–277
29. Cai Q, Brissova M, Reinert RB, et al. Enhanced expression of VEGF-A in β cells increases endothelial cell number but impairs islet morphogenesis and β cell proliferation. Dev Biol 2012;367:40–54
30. Agudo J, Ayuso E, Jimenez V, Casellas A, Mallol C, Salavert A, et al. Vascular endothelial growth factor-mediated islet hypervascularization and inflammation contribute to progressive reduction of β-cell mass. Diabetes 2012;61:2851–2861.
31. Li X, Zhang L, Meshinchi S, et al. Islet microvasculature in islet hyperplasia and failure in a model of type 2 diabetes. Diabetes 2006;55:2965–2973
32. Thurston G, Suri C, Smith K, et al. Leakage-resistant blood vessels in mice transgenically overexpressing angiopoietin-1. Science 1999;286:2511–2514
33. Nakamura M, Kitamura H, Konishi S, et al. The endocrine pancreas of spontaneously diabetic db/db mice: microangiopathy as revealed by transmission electron microscopy. Diabetes Res Clin Pract 1995;30:89–100
34. Wynn TA. Common and unique mechanisms regulate fibrosis in various fibroproliferative diseases. J Clin Invest 2007;117:524–529
35. Nikolova G, Jabs N, Konstantinova I, et al. The vascular basement membrane: a niche for insulin gene expression and Beta cell proliferation. Dev Cell 2006;10:397–405
36. Hahn C, Schwartz MA. Mechanotransduction in vascular physiology and atherogenesis. Nat Rev Mol Cell Biol 2009;10:53–62
37. Hellström M, Kalén M, Lindahl P, Abramsson A, Betsholtz C. Role of PDGF-B and PDGFR-beta in recruitment of vascular smooth muscle cells and pericytes during embryonic blood vessel formation in the mouse. Development 1999;126:3047–3055
38. Lindblom P, Gerhardt H, Liebner S, et al. Endothelial PDGF-B retention is required for proper investment of pericytes in the microvessel wall. Genes Dev 2003;17:1835–1840
39. Albrecht EWJA, Stegeman CA, Heeringa P, Henning RH, van Goor H. Protective role of endothelial nitric oxide synthase. J Pathol 2003;199:8–17
40. Ahrén B. Autonomic regulation of islet hormone secretion—implications for health and disease. Diabetologia 2000;43:393–410
41. Marino JS, Xu Y, Hill JW. Central insulin and leptin-mediated autonomic control of glucose homeostasis. Trends Endocrinol Metab 2011;22:275–285
42. Storkebaum E, Carmeliet P. Paracrine control of vascular innervation in health and disease. Acta Physiol (Oxf) 2011;203:61–86
43. Burnstock G. Autonomic neurotransmission: 60 years since sir Henry Dale. Annu Rev Pharmacol Toxicol 2009;49:1–30
44. Ahrén B, Lundquist I. Modulation of basal insulin secretion in the obese, hyperglycemic mouse. Metabolism 1982;31:172–179
45. Atef N, Brulé C, Bihoreau MT, Ktorza A, Picon L, Pénicaud L. Enhanced insulin secretory response to acetylcholine by perifused pancreas of 5-day-old preobese Zucker rats. Endocrinology 1991;129:2219–2224
46. Atef N, Ktorza A, Picon L, Pénicaud L. Increased islet blood flow in obese rats: role of the autonomic nervous system. Am J Physiol 1992;262:E736–E740
47. Moncada S. Adventures in vascular biology: a tale of two mediators. Philos Trans R Soc Lond B Biol Sci 2006;361:735–759
48. Richards OC, Raines SM, Attie AD. The role of blood vessels, endothelial cells, and vascular pericytes in insulin secretion and peripheral insulin action. Endocr Rev 2010;31:343–363
49. Weidner N. Current pathologic methods for measuring intratumoral microvessel density within breast carcinoma and other solid tumors. Breast Cancer Res Treat 1995;36:169–180
50. Ricordi C, Gray DW, Hering BJ, et al. Islet isolation assessment in man and large animals. Acta Diabetol Lat 1990;27:185–195